Computers and Electronics in Agriculture 154 (2018) 18–24

Contents lists available at ScienceDirect

Computers and Electronics in Agriculture

journal homepage: www.elsevier.com/locate/compag

Original papers

A recognition method for cucumber diseases using leaf symptom images based on deep convolutional neural network

Juncheng Ma[a], Keming Du[a,*], Feixiang Zheng[a], Lingxian Zhang[b,*], Zhihong Gong[c], Zhongfu Sun[a]

[a] Institute of Environment and Sustainable Development in Agriculture, Chinese Academy of Agricultural Sciences, Beijing 100081, China
[b] College of Information and Electrical Engineering, China Agricultural University, Beijing 100083, China
[c] Tianjin Climate Center, Tianjin 300074, China

ARTICLE INFO

Keywords:
Cucumber
Diseases
Deep convolutional neural network
Symptom images
Recognition

ABSTRACT

Manual approaches to recognize cucumber diseases are often time-consuming, laborious and subjective. A deep convolutional neural network (DCNN) was proposed to conduct symptom-wise recognition of four cucumber diseases, i.e., anthracnose, downy mildew, powdery mildew, and target leaf spots. The symptom images were segmented from cucumber leaf images captured under field conditions. In order to decrease the chance of overfitting, data augmentation methods were utilized to enlarge the datasets formed by the segmented symptom images. With the augmented datasets containing 14,208 symptom images, the DCNN achieved good recognition results, with an accuracy of 93.4%. In order to compare the results of the DCNN, comparative experiments were conducted using conventional classifiers (Random Forest and Support Vector Machines), as well as AlexNet. Results showed that the DCNN was a robust tool for recognizing the cucumber diseases in field conditions.

1. Introduction

Plant disease is a common threat to yield and quality of global agricultural production and bears responsibility for a significant portion of production costs. It is reported that the loss caused by plant disease accounts for at least a 10% reduction in global food production (Mutka & Bart, 2015). Cucumber, one of the most common vegetables in China, is severely affected by various diseases, such as downy mildew and powdery mildew (Zhang et al., 2017b; Ma et al., 2017). The process of recognizing diseases is often time consuming, laborious and subjective. Most of disease damage evaluation and treatment are done by farmers in the field with the guidance of plant pathologists. Incorrect diagnosis and pesticide usage are very common. Therefore, a timely and accurate recognition method of cucumber diseases is in great demand.

With the development of computer vision and machine learning, progress has been achieved on recognition and diagnosis of plant diseases (Bai et al., 2017; Dorj et al., 2017; Mahlein, 2016; Ma et al., 2015; Mutka & Bart, 2015; Pethybridge & Nelson, 2015; Stewart & Mcdonald, 2014; Bock et al., 2009). Many recognition and diagnosis methods are proposed by following the pipelined procedures of image segmentation, feature extraction, and pattern recognition (Zhang et al., 2017a; Zhang et al., 2017b; Du et al., 2016). Recognition methods following the pipelined procedures have made some progress. But these methods are subject to two issues. First, the accuracy of these methods greatly depends on the extraction and selection of the visible disease features. Specifically, features of visible disease symptoms should be extracted accurately and proper features should be selected. Second, the methods following the pipelined procedures are relatively complicated. The presence of noises is largely unavoidable in disease images captured under field conditions, such as uneven illumination and clutter field background. This can severely decrease the quality of the features and affect the results of recognition. Therefore, many efforts are spent on eliminating the noises in the conventional methods to achieve robust results.

Convolutional neural network (CNN) is one of the best-performing methods for image recognition (Ghazi et al., 2017; Ding & Taylor, 2016; Grinblat et al., 2016; Krizhevsky et al., 2012). CNN can automatically learn appropriate features from training datasets instead of manual feature extraction. CNN has been proven to be a good option for plant disease recognition (Ferentinos, 2018; Mohanty et al., 2016). These applications of CNN based plant diseases diagnosis have been performed leaf-wise, assuming that the symptoms on a single leaf belong to one disease. However, multiple diseases may occur simultaneously in field conditions and symptoms of different diseases can be present on the same leaf. This may significantly influence the accuracy of the leaf-wise plant disease diagnosis (Barbedo, 2016; Bock et al., 2009). The

* Corresponding authors at: Institute of Environment and Sustainable Development in Agriculture, Chinese Academy of Agricultural Sciences, 12, Zhongguancun South Street, Haidian District, Beijing 100081, China.
E-mail addresses: dukeming@caas.cn (K. Du), zhanglx@cau.edu.cn (L. Zhang).

https://doi.org/10.1016/j.compag.2018.08.048
Received 26 June 2018; Received in revised form 27 August 2018; Accepted 31 August 2018
Available online 06 September 2018

symptom-wise plant disease recognition appears therefore to be a necessary supplement.

The objective of this paper was to apply state of the art deep learning techniques to the recognition of cucumber diseases using visible leaf symptom images. A deep convolutional neural network (DCNN) was utilized to conduct symptom-wise classification so that plant disease recognition can be achieved without the influence of multiple diseases symptoms presented on one leaf. An image dataset containing symptom images of four cucumber diseases, i.e., anthracnose, downy mildew, powdery mildew and target leaf spots, was constructed. Based on the dataset, the DCNN was trained to recognize cucumber diseases.

2. Material and methods

2.1. Image datasets

The dataset used for recognition was composed of symptom images of anthracnose (*Colletotrichum orbiculare*), downy mildew (*Pseudoperonospora cubensis*), powdery mildew (*Golovinomyces cichoracearum*) and target leaf spots (*Corynespora cassiicola*). Some disease images are shown in Fig. 1. Symptom images of anthracnose, target leaf spots, and part of downy mildew were segmented from images downloaded from the Internet (PlantVillage, https://plantvillage.org/. Forestry Images, https://www.forestryimages.org/). The remaining symptom images were segmented from images captured using a digital camera (Nikon Coolpix S3100) under field conditions at the Greenhouse No.5 of the Agricultural Scientific Innovation Base, Tianjin Academy of Agricultural Sciences, Tianjin, China. Images were obtained in a 2592 × 1944 pixel spatial resolution with flash always off and without optical or digital zoom. The images were captured between 8:00 and 17:00 on April 20, 2016. All the images were resized to 800 × 600 pixels prior to image analysis to reduce the computational cost and improve the image processing efficiency.

Symptom images were segmented using a disease symptom segmentation method which combined a comprehensive color feature with region growing. The comprehensive color feature (CCF) consists of three color components, Excess Red Index (ExR), H component of HSV color space and b* component of L*a*b* color space, which implements powerful discrimination of disease spots and clutter background. Then an interactive region growing method based on the color feature was used to achieve robust and fast symptom image segmentation (Fig. 2). For more details about the method, readers are referred to Ma et al., (2017). Since the disease symptoms were small in area, all symptom images were resized to 20 × 20 × 3 for the recognition. A dataset containing 1184 symptom images was constructed. The number of symptom images for the four cucumber diseases, i.e., anthracnose, downy mildew, powdery mildew and target leaf spots, was 229, 415, 332, and 208 respectively. The constructed dataset was then divided into training and test datasets in a ratio of 8:2 by randomly selecting images from the dataset. Of the symptom images in the training dataset, 80% was used for training and 20% was used for validation.

Data augmentation can help enlarge the datasets for recognition and decrease the chance of overfitting (Barré et al., 2017; Grinblat et al., 2016). Because the datasets in this paper were relatively small, data augmentation was performed on the original datasets. Many techniques can be used for data augmentation, such as PCA jittering, random crop, image rotation and affine transformations (Dyrmann et al., 2016; Krizhevsky et al., 2012). Given the small size of the input symptom images, the augmentation method in this paper adopted transformations that would not reduce the size of input images. The augmentation method in this paper was to rotate the original datasets by 90, 180 and 270 degrees and flip horizontally and vertically. This produced 12 augmented datasets.

2.2. The deep convolutional neural network

The MatConvNet (Vedaldi & Lenc, 2015), a MATLAB (MathWorks Inc., USA) toolbox, was used to implement the CNN. The architecture of the DCNN is depicted in Fig. 3. It can be seen that an architecture similar to Lenet5 (Lecun et al., 1998) was adopted because it was fast to deploy and powerful in small-scale image recognition tasks (Ding & Taylor, 2016). Starting with the input layer formed by the symptom images in RGB color space with a size of 20 × 20 × 3, the DCNN was composed of four modules. The first module consisted of a Convolutional Layer that had 20 filters with a size of 5 × 5, and a Max-pooling Layer with the filter that had a size of 2 × 2 and a stride of 2. The Max-pooling Layer was applied to perform downsampling operations, i.e. shrinking the feature maps along both width and height by a factor of two (Barré et al., 2017). The second module consisted of a Convolutional Layer that had 100 filters with a size of 3 × 3, and a Max-pooling Layer with the filter that had a size of 2 × 2 and a stride of 2. The third module consisted of a Convolutional Layer that had 1000 filters with a size of 3 × 3. The last module of the DCNN consisted of a Fully Connected Layer with 1500 neurons. The output layer had four neurons representing the four cucumber diseases, i.e. anthracnose, downy mildew, powdery mildew and target leaf spots. Given the output layer, SoftMax function was used to calculate the estimated probability of the four categories of cucumber diseases.

The DCNN was trained on a NVIDIA Quadro P4000 (8 GB memory) with CUDA 9.0. The stochastic gradient descent with momentum (SGDM) was used to optimize the network weights. The learning rate was initialized as 0.001 and dropped every 20 epochs by a drop factor of 0.1. The momentum was set to 0.9 and remained constant for the training processing. A mini-batch of 128 was used. The maximum number of epochs used for training was set to 800.

2.3. Evaluation of the DCNN

Conventional classifiers used for the comparative tests with the DCNN were Random Forests (RF) (Breiman, 2001), and Support Vector Machines (SVM) (Cortes & Vapnik, 1995). AlexNet (Krizhevsky et al., 2012) was also adopted for comparison by transfer learning. For the conventional classifiers that were compared to the DCNN, recognition was achieved by following the pipelined procedures. After symptom image segmentation, feature extraction was performed, extracting color and texture features to distinguish the symptoms caused by different diseases. The color features consisted of the mean and variance of the nine channels from three color spaces, including R, G, B from RGB color space, H, S, V, from HSV color space, and L, a*, b*, from CIEL*a*b*

(a) Anthracnose (b) Downy mildew (c) Powdery mildew (d) Target leaf spots

Fig. 1. Images of the four cucumber diseases.

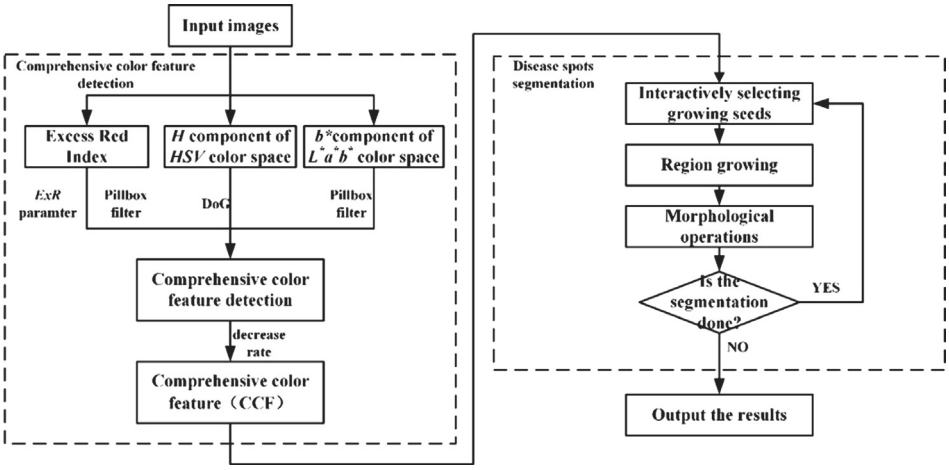

Ma et al., 2017.

Fig. 2. General scheme for the disease symptom segmentation (Ma et al., 2017).

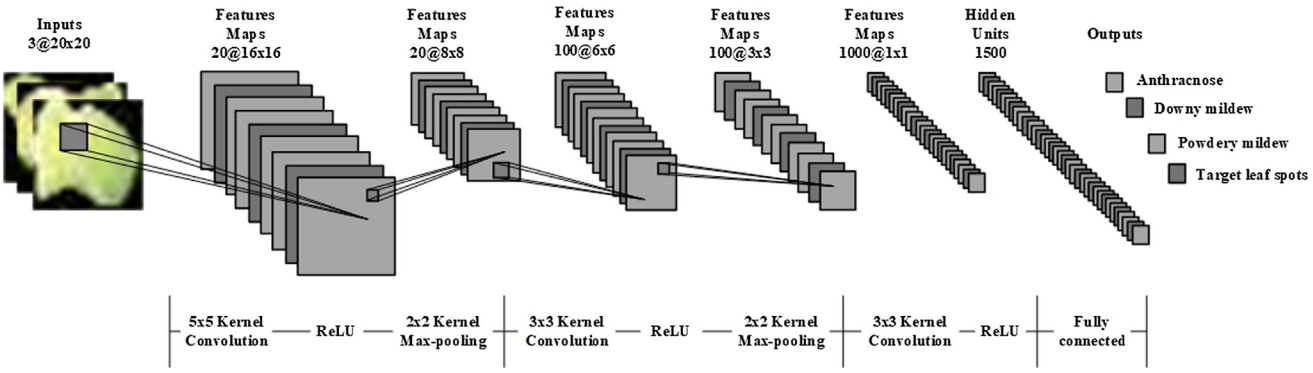

Fig. 3. The architecture of the DCNN model.

color space. The texture features were calculated from the Gray-level co-occurrence matrix of each channel, including contrast, correlation, energy and homogeneity of the nine channels. A feature set containing 54 features was conducted.

Confusion matrices were used to compare the classifierss' performance. Each row of the confusion matrix represented the instances in a predicted cucumber disease while each column represented the instances in an actual cucumber disease (Powers, 2011). Based on the confusion matrix, three metrics, Precision, Sensitivity, and F1 score were used to evaluate the performances of the methods.

$$\text{Sensitivity} = \frac{\text{number of correctly predicted}}{\text{total number of true cases}} \quad (1)$$

$$\text{Precision} = \frac{\text{number of correctly predicted}}{\text{total number of predictions}} \quad (2)$$

$$\text{F1 score} = 2*\frac{\text{Sensitivity} * \text{Precision}}{\text{Sensitivity} + \text{Precision}} \quad (3)$$

3. Results and discussion

3.1. Cucumber diseases recognition

Data augmentation scheme was performed to training dataset and test dataset respectively. An augmented dataset containing 14,208 symptom images was constructed. The number of images in the three datasets was 8628, 2292, and 3288 respectively (Table 1).

The test results were shown in Table 2. It can be seen from the confusion matrix the DCNN achieved an accuracy of 93.4%, indicating that most of the predicted samples and the true values match. In the performance per class, the best performance was achieved by the DCNN on the class downy mildew (F1 = 97.0). Out of 1100 downy mildew predictions, 96.7% were correct. Similar recognition results can be observed on the class powdery mildew. 98.2% of 1006 predictions of powdery mildew were correctly classified. The predictive accuracy for class anthracnose and target leaf spots was 82.0% and 91.8% respectively. As expected, the DCNN demonstrated superior results on the class downy mildew and powdery mildew, since the number of data in these two classes was larger than that in the other classes. In order to ensure if the number of data was an influence of factor to the DCNN, an experiment was performed on the DCNN with balanced data.

Table 1
Statistics of the datasets used for the construction of the model.

Disease	Original dataset	Augmented dataset	Training	Validation	Test
Anthracnose	229	2748	1716	432	600
Downy mildew	415	4980	3108	780	1092
Powdery mildew	332	3984	2352	588	1044
Target leaf spots	208	2496	1452	492	552
Total	1184	14,208	8628	2292	3288

For this experiment, 1600 symptom images were randomly selected from each class in the augmented training dataset, as well as 400 symptom images from each class in the augmented test dataset, so that all classes contained the same number of images. In this manner, a dataset containing 8000 symptom images was constructed, of which

Table 2
Confusion matrix of the DCNN with unbalanced data.

Disease	Anthracnose	Downy mildew	Powdery mildew	Target leaf spots	Precision (%)	Sensitivity (%)	F1 score
Anthracnose	559	1	43	79	82.0	93.2	87.2
Downy mildew	10	1064	13	13	96.7	97.4	97.0
Powdery mildew	12	5	988	1	98.2	94.6	96.4
Target leaf spots	19	22	0	459	91.8	83.2	87.3
Accuracy (%)	93.4						

Table 3
Confusion matrix of the DCNN with balanced data.

Disease	Anthracnose	Downy mildew	Powdery mildew	Target leaf spots	Precision (%)	Sensitivity (%)	F1 score
Anthracnose	371	1	14	56	83.9	92.8	88.1
Downy mildew	8	386	3	8	95.3	96.5	95.9
Powdery mildew	8	2	383	0	97.5	95.8	96.6
Target leaf spots	13	11	0	336	93.3	84.0	88.4
Accuracy (%)	92.2						

5120 were used for training, 1280 for validation and 1600 for test. Table 3 showed the confusion matrix of the DCNN with balanced data.

As expected, the performance of the DCNN showed a degradation on the accuracy compared to that with unbalanced data. The results indicated that the number of data in the input dataset was an influence of factor to the DCNN, which agreed with the conclusion that the DCNN can achieve satisfactory results with a large mass of data. In the performance per class, the best performance was achieved by the DCNN on class powdery mildew (F1 = 96.6). 97.5% of 393 predictions of powdery mildew were correctly classified. The performance of the DCNN on class downy mildew and powdery mildew was still better than that on class anthracnose and target leaf spots even though the same number of symptom images was used for each class. The sensitivity value for each class was 92.8, 96.5, 95.8, and, 84.0 respectively, indicating that the DCNN made more errors predicting class anthracnose and target leaf spots. Out of 400 anthracnose cases, 92.8% were correctly classified. In terms of the 400 cases of target leaf spots, only 84.0% were correctly predicted. This may be caused by the reasons that symptom images of class anthracnose and target leaf spots were segmented from images downloaded from the Internet. These disease images may be processed for screen display so that the original information presented by disease symptoms was inaccessible by the DCNN. In contrast, symptom images of class downy mildew and powdery were mainly segmented from images without special process. Based on the results, it could be concluded that the quality of the dataset was also an influence of factor to the DCNN.

In order to show the effectiveness of data augmentation for the performance of the DCNN, experiments on the DCNN with datasets augmented by different augmentation methods were conducted. Four input datasets were established, i.e., no augmentation, rotation augmentation only, flip augmentation only and both rotation and flip augmentation. Recognition accuracy was adopted as the evaluation metric. The results were shown in Table 4. It was revealed the accuracy of the DCNN over the four datasets was 86.8%, 89.8%, 91.6%, and 93.4% respectively. Both rotation augmentation and flip augmentation improved the performance compared to no augmentation. The best performance was achieved by the DCNN on dataset both rotation and flip augmentation. Using both rotation and flip augmentation, the performance of the DCNN improved significantly, i.e. from 86.8% to 93.4%. Therefore, to achieve better recognition, it was necessary to perform data augmentation prior to CNN training.

In order to demonstrate the robustness of the DCNN to the illumination in field conditions, a dataset containing 636 symptom images of downy mildew under the influence of illumination was constructed by data augmentation scheme. The symptom images in the dataset were not utilized in the construction of the DCNN (Fig. 4).

The DCNN was tested on the dataset and the results were shown in Table 5. It can be seen that 624 cases of downy mildew were correctly recognized, indicating that the DCNN achieved an accuracy of 98.1%. The results showed that the DCNN was able to recognize symptom images under the influence of illumination.

3.2. Performance evaluation

The performance of the pretrained network, AlexNet, was tested by transfer learning in this section. The learned features by AlexNet were transferred to the new task of cucumber disease recognition. The training parameters used for AlexNet were same to the aforementioned DCNN. Table 6 showed the performance of AlexNet by transferring learning.

The results presented in Table 6 indicated that AlexNet achieved better performances than the DCNN. The accuracy of AlexNet with the two datasets was 94.0% and 92.6% respectively. As expected, AlexNet by transfer learning outperformed the DCNN trained from scratch, which may be caused by the reasons that AlexNet has been trained over a million images, therefore, the feature presentations were much richer than that of the DCNN trained from scratch.

Prior to training of the conventional classifiers, Pearson's Rank correlations were conducted between pairs. The absolute values of pairwise Pearson's Rank correlations for 54 features were calculated and ranked. The features with the highest average rank were considered for removal first. Then, according to the contributions to the classification, the choice of which of the two features to drop was determined. Features were reduced until all the Pearson's Rank correlation coefficients for the features pairs were below $|0.7|$, which resulted in a feature subset containing 20 features (Table 7).

The conventional classifiers were built based on the 20 selected features. Disease recognition was achieved by the classifiers over the

Table 4
Effectiveness of data augmentation.

	No augmentation	Rotation augmentation	Flip augmentation	Both rotation and flip augmentation
Accuracy	86.8%	89.8%	91.6%	93.4%

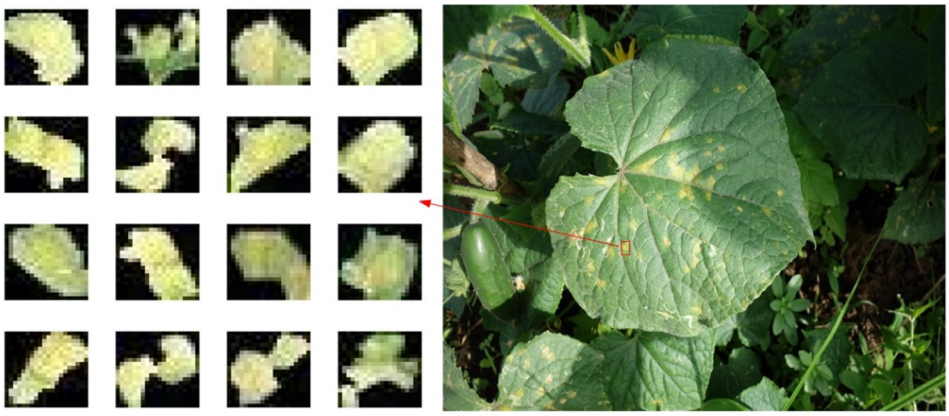

Fig. 4. Symptom images under the influence of illumination.

Table 5
Test results of the DCNN on symptom images under the influence of illumination.

Disease	Anthracnose	Downy mildew	Powdery mildew	Target leaf spots
Downy mildew	3	624	6	3
Accuracy (%)	98.1			

balanced dataset. Results were shown in Table 8.

It was revealed in Table 8 the accuracy of the conventional classifiers, i.e., SVM and RF, was 81.9% and 84.8% respectively. Compared to the conventional classifiers, the DCNN demonstrated superior results of recognition accuracy. In the performance per class, similar to the DCNN, the conventional classifiers performed better on the class downy mildew and powdery mildew, which agreed with the conclusions that the quality of the dataset was an influence of factor. Although the DCNN showed similar ability to RF on recognizing class downy mildew and powdery mildew, the DCNN outperformed RF on class anthracnose and target leaf spots, indicating that the DCNN was more tolerant to the quality of the dataset.

3.3. Disease recognition in field conditions

Since the DCNN have achieved robust recognition results, it was adopted in the experiments on disease recognition in field conditions. In order to test if the DCNN was robust to image sensors, disease images used in this experiment were captured using a smart phone (iPhone six plus) at the Greenhouse No. 1–4 of Tianjin climate center, Tianjin, China. The images were captured between 15:00 and 17:00 on April 27, 2018. By following the same protocols for image capture as in the DCNN construction, the images were captured in a 2448 × 3264 pixel spatial resolution. Disease recognition results were achieved by combining the symptom image segmentation and the DCNN based recognition. Fig. 5 showed some recognition results of randomly selected images.

Symptom images were segmented from the disease images (top left) captured in field conditions by interactively selecting growing seeds. The DCNN was used to classify the segmented symptom images, as well as to calculate the class probabilities (bottom left). The histogram demonstrated the four predicted diseases and the associated probabilities (bottom right). The disease labels were sorted based on the probabilities. The results showed the DCNN achieved excellent recognition results in conjunction with the symptom image segmentation method, indicating that the method had a good potential to be extended to field use by combining with mobile devices. The future work will be focusing on this mobile device-based recognition system combining with an expert system that was capable of making decisions like a human expert. This recognition system can make a reliable tool for both plant pathologists and farmers, which will help save human efforts and reduce pesticide usage. At the same time, efforts will be spent on deepening the convolutional network to obtain more accurate image

Table 7
Features used for the construction of the conventional classifiers.

Channels	Features
G of RGB color space	Average, contrast, correlation, energy, homogeneity
H of HSV color space	Average, contrast, correlation, energy
S of HSV color space	Contrast, correlation, homogeneity
a^* of CIEL*a*b* color space	Average, variance, correlation, energy
b^* of CIEL*a*b* color space	Average, contrast, energy
L^* of CIEL*a*b* color space	Contrast

Table 6
Confusion matrix of the pretrained networks with unbalanced data.

Disease	Anthracnose	Downy mildew	Powdery mildew	Target leaf spots	Precision (%)	Sensitivity (%)	F1 score
AlexNet with unbalanced data							
Anthracnose	547	0	23	77	84.5	91.2	87.7
Downy mildew	4	1066	0	4	99.3	97.6	98.4
Powdery mildew	35	5	1020	14	95.0	97.7	96.3
Target leaf spots	14	21	1	457	92.7	82.8	87.5
Accuracy (%)	94.0						
AlexNet with balanced data							
Anthracnose	368	0	16	49	85.0	92.0	88.4
Downy mildew	7	386	0	7	96.5	96.5	96.5
Powdery mildew	8	2	384	0	97.5	96.0	96.7
Target leaf spots	17	12	0	344	92.2	86.0	89.0
Accuracy (%)	92.6						

Table 8
Confusion matrix of the conventional classifiers with balanced data.

Disease	Anthracnose	Downy mildew	Powdery mildew	Target leaf spots	Precision (%)	Sensitivity (%)	F1 score
SVM with balanced data							
Anthracnose	332	7	131	49	64.0	83.0	72.3
Downy mildew	0	368	0	10	97.4	92.0	94.6
Powdery mildew	4	0	269	0	98.5	67.3	80.0
Target leaf spots	64	25	0	341	79.3	85.3	82.2
Accuracy (%)	81.9						
RF with balanced data							
Anthracnose	339	0	6	95	77.0	84.8	80.7
Downy mildew	0	374	3	30	91.9	93.5	92.7
Powdery mildew	3	3	385	17	94.4	96.3	95.3
Target leaf spots	58	23	6	258	74.8	64.5	69.3
Accuracy (%)	84.8						

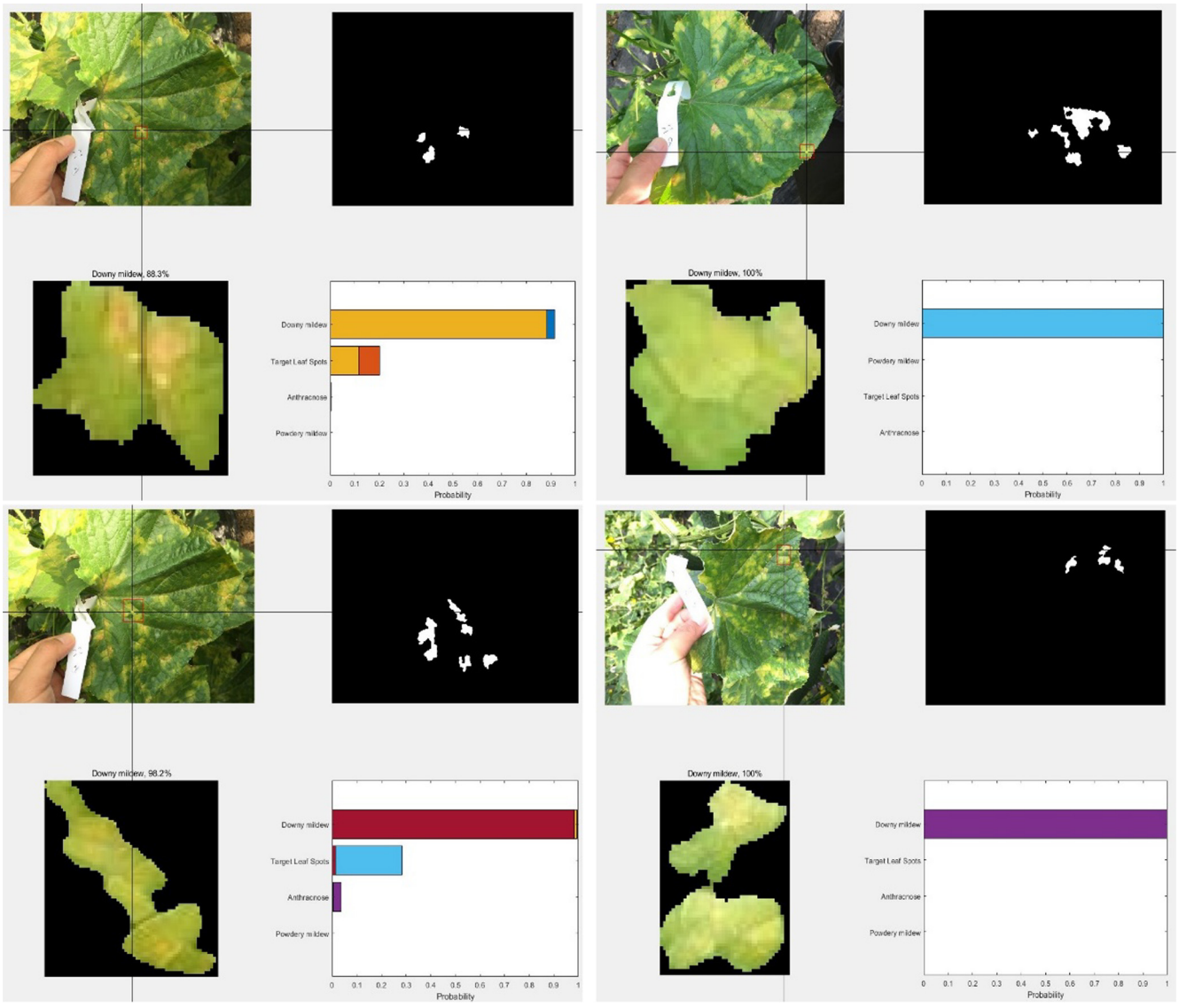

Fig. 5. Recognition results of cucumber diseases in field conditions.

recognition results. Recognizing multiple types of diseases will be another important extension. The dataset will be enlarged to cover as many variabilities occurred in practice as possible. In order to detect and recognize the diseases at early stages, hyperspectral imaging and thermal infrared imaging will be incorporated in the following work.

4. Conclusion

A deep convolutional neural network was proposed to conduct symptom-wise recognition of cucumber diseases. The symptom images were segmented from cucumber leaf images captured in field conditions by an image segmentation method which implemented powerful

discrimination of disease symptoms and clutter background. Based on the symptom images, a dataset containing 4 diseases, i.e., anthracnose, downy mildew, powdery mildew, and target leaf spots was constructed, which was then augmented by data augmentation method. Quantitative experiments demonstrated that the DCNN achieved excellent recognition results. The accuracy of the DCNN on the unbalanced dataset and balanced dataset was 93.4% and 92.2% respectively. Comparative tests showed AlexNet outperformed the DCNN due to its rich feature presentations. Both the DCNN and AlexNet showed superior results to the conventional classifiers.

Acknowledgments

The research presented in this paper was supported by Beijing Leafy Vegetables Innovation Team of Modern Agro-industry Technology Research System (BAIC07-2018) and Key Laboratory of Agricultural Informatization Standardization, Ministry of Agriculture and Rural Affairs, China (AIS2018-01).

Appendix A. Supplementary material

Supplementary data associated with this article can be found, in the online version, at https://doi.org/10.1016/j.compag.2018.08.048.

References

Bai, X., Li, X., Fu, Z., Lv, X., Zhang, L., 2017. A fuzzy clustering segmentation method based on neighborhood grayscale information for defining cucumber leaf spot disease images. Comput. Electron. Agric. 136, 157–165.
Barbedo, J.G.A., 2016. A review on the main challenges in automatic plant disease identification based on visible range images. Biosyst. Eng. 144, 52–60.
Barré, P., Stöver, B.C., Müller, K.F., Steinhage, V., 2017. LeafNet: a computer vision system for automatic plant species identification. Ecol. Inf. 40, 50–56.
Bock, C.H., Cook, A.Z., Parker, P.E., Gottwald, T.R., 2009. Automated image analysis of the severity of foliar citrus canker symptoms. Plant Dis. 93, 660–665.
Breiman, L., 2001. Random forests. Machine Learn. 45 (1), 5–32.
Cortes, C., Vapnik, V., 1995. Support-vector networks. Machine Learn. 20 (3), 273–297.
Ding, W., Taylor, G., 2016. Automatic moth detection from trap images for pest management. Comput. Electron. Agric. 123, 17–28.
Dorj, U.-O., Lee, M., Yun, S., 2017. An yield estimation in citrus orchards via fruit detection and counting using image processing. Comput. Electron. Agric. 140, 103–112.
Du, K., Sun, Z., Li, Y., Zheng, F., Chu, J., Su, Y., 2016. Diagnostic model for wheat leaf conditions using image features and a support vector machine. Trans. ASABE 59, 1041–1052.
Dyrmann, M., Karstoft, H., Midtiby, H.S., 2016. Plant species classification using deep convolutional neural network. Biosyst. Eng. 151, 72–80.
Ferentinos, K.P., 2018. Deep learning models for plant disease detection and diagnosis. Comput. Electron. Agric. 145, 311–318.
Ghazi, M.M., Yanikoglu, B., Aptoula, E., 2017. Plant identification using deep neural networks via optimization of transfer learning parameters. Neurocomputing 235, 228–235.
Grinblat, G.L., Uzal, L.C., Larese, M.G., Granitto, P.M., 2016. Deep learning for plant identification using vein morphological patterns. Comput. Electron. Agric. 127, 418–424.
Krizhevsky, A., Sutskever, I., Hinton, G.E., 2012. ImageNet classification with deep convolutional neural networks. Adv. Neural Inform. Process. Sys. 1–9.
Lecun, Y., Bottou, L., Bengio, Y., Haffner, P., 1998. Gradient-based learning applied to document recognition. Proc. IEEE 86 (11), 2278–2324.
Ma, J., Du, K., Zhang, L., Zheng, F., Chu, J., Sun, Z., 2017. A segmentation method for greenhouse vegetable foliar disease spots images using color information and region growing. Comput. Electron. Agric. 142, 110–117.
Ma, J., Li, X., Wen, H., Fu, Z., Zhang, L., 2015. A key frame extraction method for processing greenhouse vegetables production monitoring video. Comput. Electron. Agric. 111, 92–102.
Mahlein, A.K., 2016. Plant disease detection by imaging sensors-parallels and specific demands for precision agriculture and plant phenotyping. Plant Dis. 100, 1–11.
Mohanty, S. P., Hughes, D., Salathe, M.. Inference of Plant Diseases from Leaf Images through Deep Learning. arXiv1604.03169 [cs]; 2016 1–6.
Mutka, A.M., Bart, R.S., 2015. Image-based phenotyping of plant disease symptoms. Front. Plant Sci. 5, 1–8.
Pethybridge, S.J., Nelson, S.C., 2015. Leaf Doctor: A new portable application for quantifying plant disease severity. Plant Dis. 99, 1310–1316.
Powers, D.M.W., 2011. Evaluation: from precision, recall and f-factor to roc, informedness, markedness & correlation. J. Machine Learn. Technol. 2 (1), 37–63.
Stewart, E.L., Mcdonald, B.A., 2014. Measuring quantitative virulence in the wheat pathogen zymoseptoria tritici using high-throughput automated image analysis. Phytopathology 104, 985–992.
Vedaldi, A., Lenc, K. MatConvNet - convolutional neural networks for MATLAB, Proc. of the ACM Int. Conf. on Multimedia; 2015.
Zhang, S., Wu, X., You, Z., Zhang, L., 2017a. Leaf image based cucumber disease recognition using sparse representation classification. Comput. Electron. Agric. 134, 135–141.
Zhang, S., Zhu, Y., You, Z., Wu, X., 2017b. Fusion of superpixel, expectation maximization and PHOG for recognizing cucumber diseases. Comput. Electron. Agric. 140, 338–347.